



(RESEARCH ARTICLE)



## Monte Carlo simulation of irradiation-induced damage in 3C-SiC and 6H-SiC using JA-IPU Code

Ambika Tundwal<sup>1,\*</sup> and Vinod Kumar<sup>2</sup>

<sup>1</sup> Department of Applied Sciences, Guru Tegh Bahadur Institute of Technology, New Delhi, India.

<sup>2</sup> University School of Basic and Applied Sciences, Guru Gobind Singh Indraprastha University, New Delhi, India.

International Journal of Science and Research Archive, 2024, 13(02), 2004–2014

Publication history: Received on 26 October 2024; revised on 02 December 2024; accepted on 05 December 2024

Article DOI: <https://doi.org/10.30574/ijrsra.2024.13.2.2382>

### Abstract

The JA-IPU code, employing the Monte Carlo technique, has been utilized to simulate damage induced in 3C-SiC and 6H-SiC. Recoils of silicon and carbon atoms, with energies ranging from 0.25 keV to 50 keV, have been imparted on these SiC polytypes. Displacement cascades have been generated up to eight generations, considering four distinct threshold energies for silicon-silicon, silicon-carbon, carbon-carbon, and carbon-silicon collisions. The results reveal that carbon interstitials and vacancies predominate over silicon interstitials and vacancies in both SiC polytypes. Additionally, damage production efficiency diminishes as the recoil energy of silicon and carbon increases. For 3C-SiC, the damage production efficiency was evaluated under two conditions: with the inclusion of electronic energy loss (EEL) and without EEL. The findings indicate that the efficiency is slightly higher in the absence of EEL.

**Keywords:** Monte Carlo technique; Threshold displacement energy; Primary knock-on atom 'PKA'; Displacement cascade; Damage production efficiency

### 1. Introduction

Silicon Carbide (SiC) polytypes are considered promising materials for use in advanced nuclear systems such as high-temperature gas reactors (HTGR), advanced nuclear fuel, and fusion reactors. In tri-iso structural (TRISO) coated fuel particle, a cladding of  $\beta$ -SiC over the fuel kernel serves to prevent the release of fission products (1). SiC's attributes, including its low activation, high thermal conductivity, chemical inertness, and high mechanical strength, make it an ideal candidate for structural components in fusion reactors (2). Despite its technological importance, it is crucial to have a fundamental understanding of the irradiation-induced damage in SiC, as such damage will impact its performance.

The production and evolution of irradiation-induced damage, as well as crystal to amorphous transformations caused by electrons and ions, have been experimentally studied in SiC (3-8). Despite numerous investigations using various analytical techniques to estimate the ion-induced damage in SiC (9, 10), computer simulations are essential for a comprehensive understanding of atomic-scale damage generated by ion-solid interactions. Consecutively, extensive efforts have been made to interpret the atomic-scale damage produced in  $\beta$ -SiC using molecular dynamics (MD) simulations (11-15). One key parameter related to damage production is the threshold displacement energy, which can be determined experimentally or estimated through MD simulations. These studies report a wide range of threshold displacement energy values ( $E_d$ ) from 20 eV to 106 eV with some uncertainty regarding the specific sublattice type due to the polytopic nature of SiC.

In the present work,  $\alpha$ -SiC and  $\beta$ -SiC out of more than 250 polytypes of SiC have been selected to study the damage induced by Si and C primary knock atom (PKA) using JA-IPU Monte Carlo code [16]. The displacement cascade has been

\* Corresponding author: Ambika Tundwal

produced for PKA energies ranging from 0.25 keV to 50 keV, similar to PKA energy spectra in SiC caused by a fission neutron spectrum. The electronic energy losses (EEL) have been incorporated into the JA-IPU code along with the lattice structure of the target material. Moreover, four different  $E_d$  values have been chosen for four possible interactions: silicon-silicon (Si-Si), silicon-carbon (Si-C), carbon-carbon (C-C) and carbon-silicon (C-Si) in SiC.

## 2. Simulation scheme

Among more than 250 polytypes of SiC, the 6H-SiC and 3C-SiC known respectively as  $\alpha$ -SiC and  $\beta$ -SiC, hold significant technological importance.  $\alpha$ -SiC has a hexagonal structure, similar to wurtzite, with lattice constant  $a = b = 3.079 \text{ \AA}$  and  $c = 15.12 \text{ \AA}$ . On the other hand,  $\beta$ -SiC has a zinc blend crystal structure with a lattice constant  $a = b = c = 4.3596 \text{ \AA}$ . The target box with dimensions  $25a \times 25b \times 50c$  has been generated by cascading the unit cells. The JA-IPU code follows the fundamental principle of binary collision, which states that the energy transferred to an initially stationary atom must exceed the threshold displacement energy ( $E_d$ ) to produce damage within the crystalline target. However, the elastic interaction between projectile and interacting atom is not governed by any specific potential.

For simulation of displacement cascade, the threshold displacement energy of the material is the most crucial parameter. This energy can be obtained through experiments, or predicted using molecular dynamics. There are four types of possible interactions: Si-Si, Si-C, C-Si, C-C. The displacement energies for these interactions may vary, and the effective displacement energies can be derived from the maximum energy transferred to the recoiled atom.

$$E_{max} = \frac{4M_1M_2}{(M_1 + M_2)^2} E$$

From the above relation, the calculated effective displacement energies using the threshold energies 20 eV for C and 40 eV for Si recommended by Zinkle and Kinoshita (17) have been given in Table 1.

**Table 1** Effective threshold displacement energies for four possible interactions

Interaction	$M_1$	$M_2$	$E_d$	$\frac{4M_1M_2}{(M_1 + M_2)^2}$	$E_d^{eff}$
Si-Si	28.086	28.086	40	1	40
Si-C	28.086	12.011	20	0.84	24
C-Si	12.011	28.086	40	0.84	48
C-C	12.011	12.011	20	1	20

These four threshold displacement energies have been adopted in the present studies to simulate the damage cascade. Based on these four displacement energies, atom + atom collision cross-sections have been calculated using the IOTA code (18) and plotted in Fig. 1 for PKA energies ranging from 0.25 keV to 50 keV.

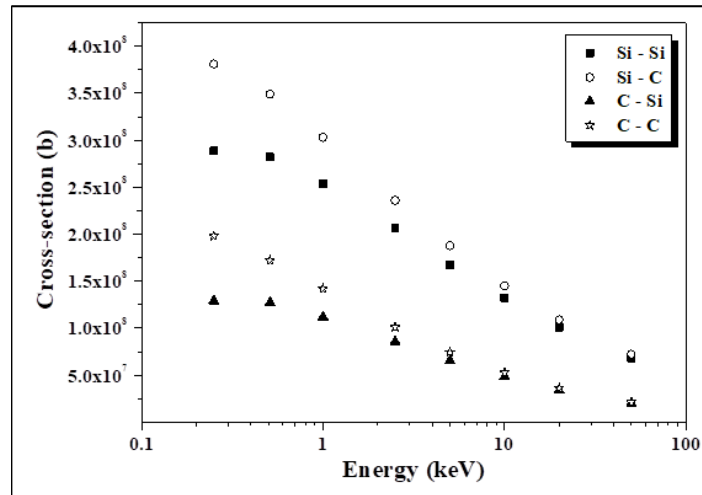


**Figure 1** Four different cross-sections for four types of possible interactions (Si-Si, Si-C, C-Si and C-C) in SiC as function of PKA Energy (keV)

### 3. Results and discussion

#### 3.1. Cascade Simulation

The damage states produced by 50 keV Si in 3C-SiC are plotted in Fig. 2 (a). In the figure, interstitials are represented by large spheres and vacancies by smaller ones, as indicated in the legend. Vacancies are defined as lattice sites that have no atoms within  $0.75 \text{ \AA}$ , while in case of interstitials, both displaced and defects are considered. An atom is said to be displaced if it moves more than  $0.75 \text{ \AA}$  from its original position; otherwise, it is classified as defect (16). In this study, only 5 Si PKA of 50 keV was injected from the origin (0,0,0) along the [1 3 5] direction. As illustrated in Fig. 2 (a), a PKA produces several branches through successive collisions along its path, resulting in distinct damaged regions separated from each other.

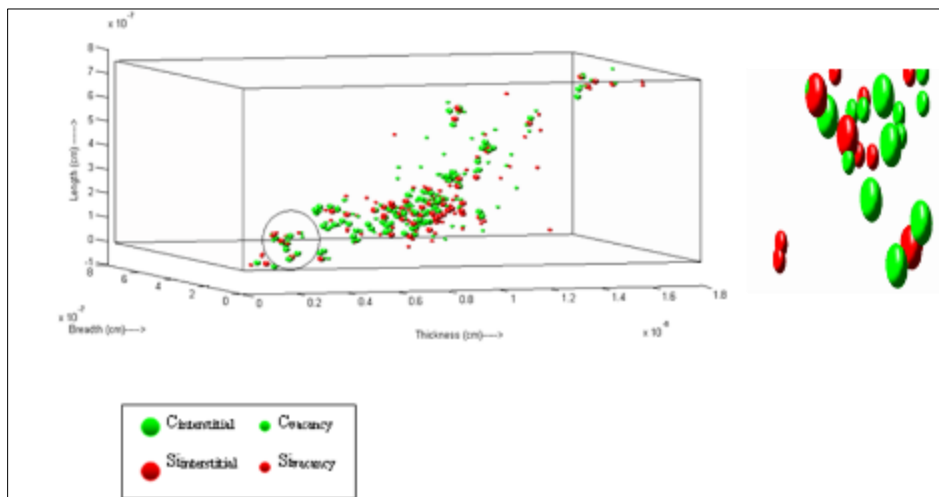


**Figure 2** (a) Illustration of a 50 keV Si cascade in 3C-SiC, (b) the damage distribution in a small region indicated in the plot (a). The damage type is distinguished by size and colour

#### 3.2. Damage production

The damage produced in both SiC polytypes (3C-SiC and 6H-SiC) has been studied using cascade simulations of 1000 Si and C PKAs with energies 0.25, 0.5, 1, 2.5, 5, 10, 20 and 50 keV. For each energy, 1000 recoil directions were selected randomly. The numbers of Si interstitials and C interstitials produced by Si PKAs and C PKAs are shown in Figs. 3 (a) and (b) for 3C-SiC and in Figs. 4 (a) and (b) for 6H-SiC.

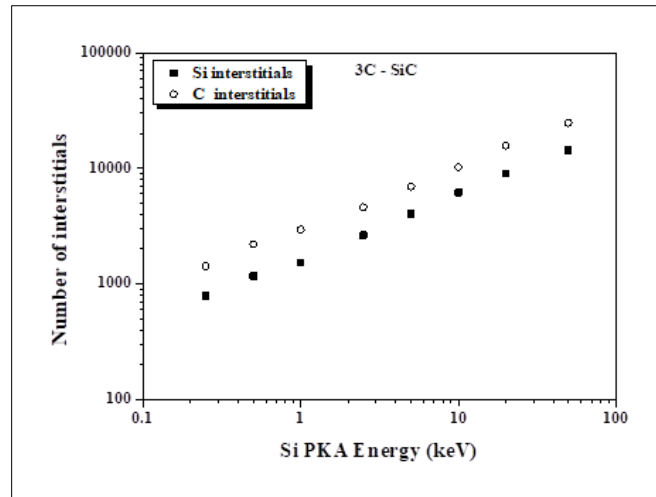


Figure 3 (a) Number of Si and C interstitials as a function of Si PKA energy

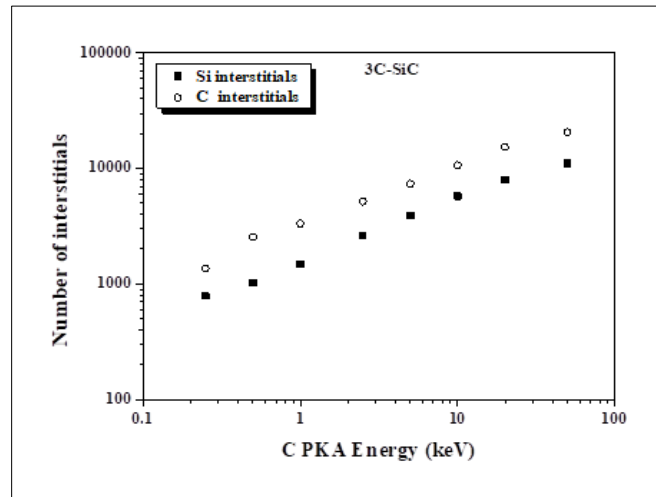


Figure 3 (b) Number of Si and C interstitials as a function of C PKA energy in case of 3C-SiC

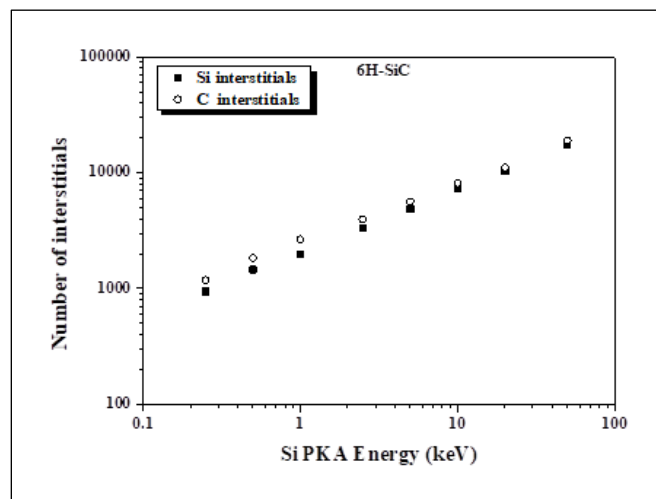
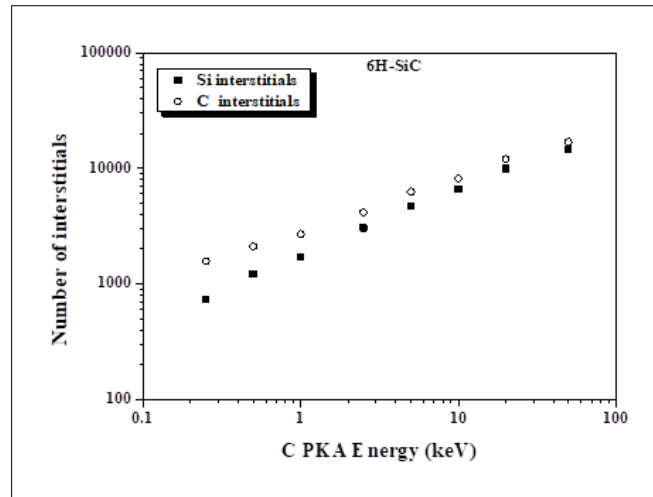


Figure 4 (a) Number of Si and C interstitials as a function of Si PKA energy



**Figure 4 (b)** Number of Si and C interstitials as a function of C PKA energy in case of 6H-SiC

It is evident from both sets of figures that C interstitials outnumbered the Si interstitials in both polytypes. However, in case of 6H-SiC, the ratio of C to Si interstitials is relatively smaller than 3C-SiC. This difference may be attributed to their lattice structures. The atomic packing fraction of 6H-SiC is greater than that of 3C-SiC. In 6H-SiC, the nearest Si-Si atom distance (3.079 Å) is smaller than 3C-SiC (3.559 Å), while Si-C distance (1.89 Å) is larger than 3C-SiC (1.09 Å). This could lead to a higher number of Si interstitials and a lower number of C interstitials in 6H-SiC compared to 3C-SiC.

Figs. 5 (a) and (b) show that the number of Si interstitials is greater and the number of C interstitials is smaller in 6H-SiC than in 3C-SiC. It should be noted that, instead of choosing half the nearest neighbour criteria, a fixed cut off distance of 0.75 Å was used for both polytypes as well as for metals in JA-IPU code.

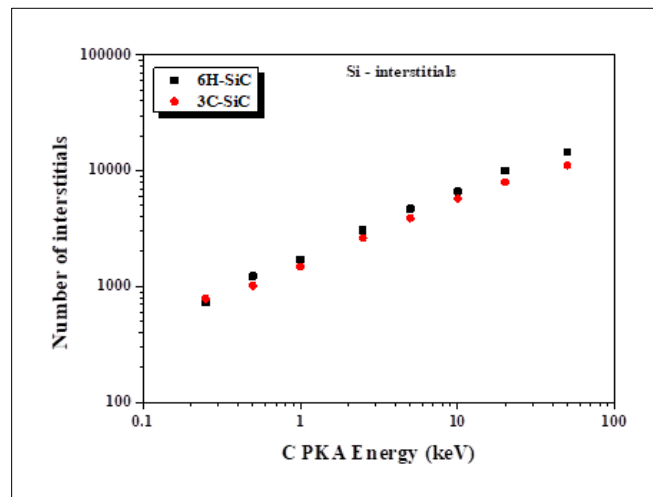


**Figure 5 (a)** Number of Si as a function of C PKA energy in both SiC polytypes

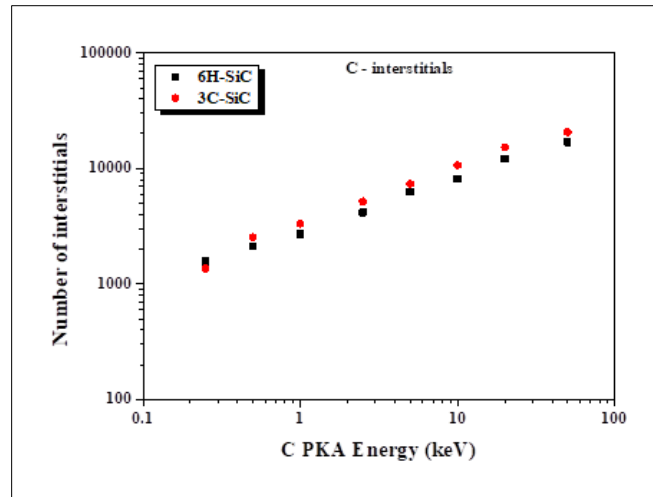


**Figure 5 (b)** Number of C interstitials as a function of C PKA energy in both SiC polytypes

The number of Si and C vacancies produced by C PKAs is shown in Figs. 6 (a) and (b) as a function of energy for 3C-SiC and 6H-SiC, respectively. For C PKAs, the C vacancies outnumber the Si vacancies by a factor of about 2 in 3C-SiC while in 6H-SiC, this ratio is about 1.67. The vacancies produced by Si PKAs in both 3C-SiC and 6H-SiC also show similar trends. Although C vacancies and interstitials are greater in number than the Si vacancies and interstitials, the values are lower than previously reported values (14). In the present study, four different threshold displacement energies have been used for the four different types of collisions.

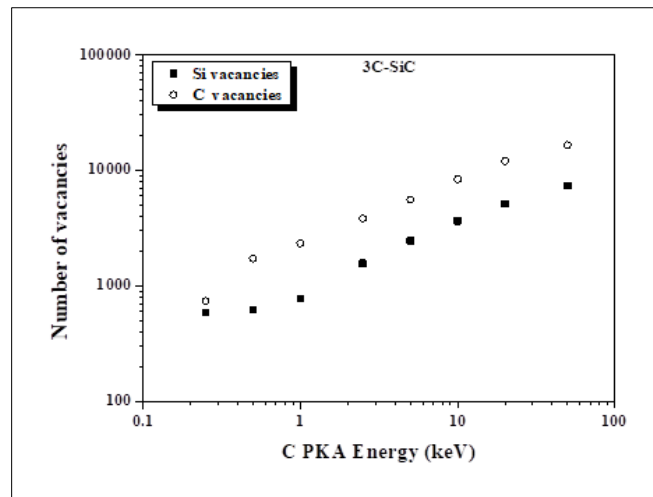


**Figure 6 (a)** Number of Si and C vacancies as a function of C PKA energy in 3C- SiC

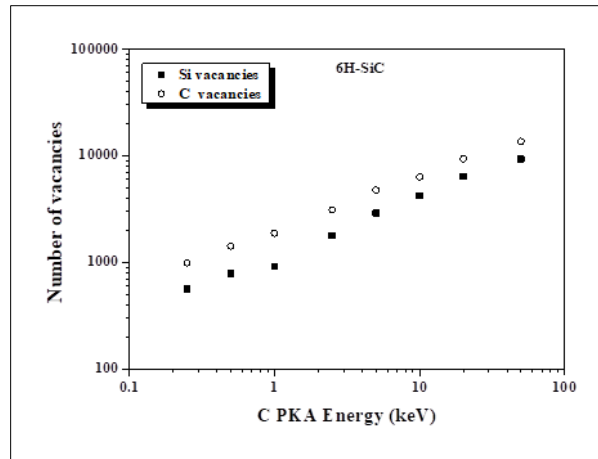


**Figure 6 (b)** Number of Si and C vacancies as a function of C PKA energy in 6H- SiC

In Figs. 7 (a) and (b), the total number of damaged atoms produced by four different types of interaction (Si-Si, Si-C, C-Si, C-C) are plotted as a function of Si PKA energy in both the SiC polytypes. The number of damaged atoms in Si-Si and Si-C interactions increases gradually with increasing Si PKA energy, while a significant change is observed in the number of damaged atoms produced by C-Si and C- C interactions.

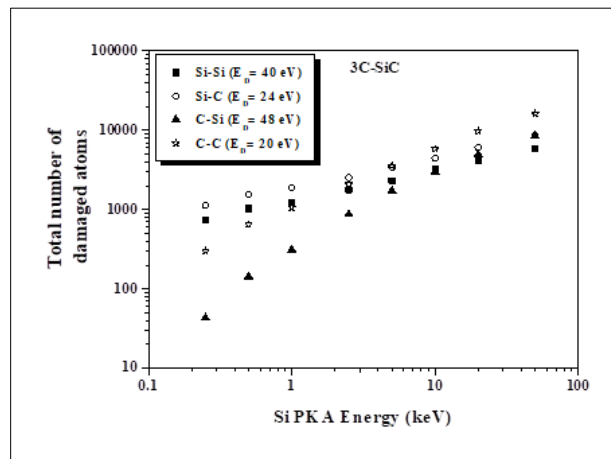


**Figure 7 (a)** Total Number of damaged atoms as a function of Si PKA energy in 3C- SiC

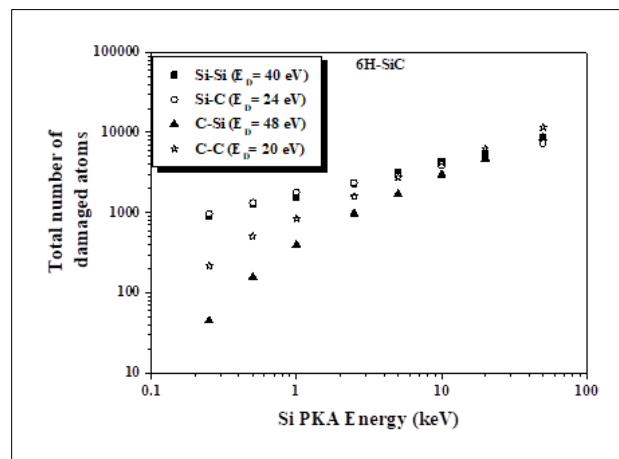


**Figure 7 (b)** Total Number of damaged atoms as a function of Si PKA energy in 6H- SiC

This may be attributed to the C-Si and C-C interaction cross-sections as shown in Fig. 1. In the case of Si PKAs, the dominant interaction is the Si-C interaction, which will produce more C as secondary recoils. The resulting C recoils further interact with Si or C atoms, and since the C-C interaction cross-section is higher than C-Si interaction cross-section, more C recoils will be created. This process continues, leading to a substantial increase in the number of damaged atoms due to C-C and C-Si interactions.

### 3.3. Damage Production Efficiency

The number of damaged atoms produced in a displacement cascade is an important parameter for radiation damage models and is estimated using the Norgett, Robison, and Torrens (NRT) formula (19), given by:

$$N_{\text{NRT}} = (0.8T_{\text{dam}}) / (2E_d)$$

where,  $T_{\text{dam}}$  is the energy of primary recoil atom (PKA) minus the energy lost in electronic energy loss and  $E_d$  is the average threshold displacement energy. In the NRT formula,  $T_{\text{dam}}$  is typically set as the PKA energy. For Si, a threshold energy  $E_d$  of 40 eV is assumed, while for C, it is 20 eV. The calculated damage production efficiency is presented in Table 2 for both SiC polytypes based on these assumptions.

**Table 2:** The average number of damaged atoms,  $N_d$ , and the damage production efficiency,  $\eta$ , produced by Si PKA and C PKA in 3C-SiC and 6H-SiC

	Si PKA				C PKA			
	3C-SiC		6H-SiC		3C-SiC		6H-SiC	
$E_{\text{PKA}}$	$N_d$	$\eta$	$N_d$	$\eta$	$N_d$	$\eta$	$N_d$	$\eta$
0.25	2.21	0.88	2.12	0.85	2.14	0.43	2.30	0.46
0.5	3.37	0.67	3.29	0.66	3.57	0.36	3.34	0.33
1	4.48	0.45	4.60	0.46	4.81	0.24	4.40	0.22
2.5	7.27	0.29	7.24	0.29	7.79	0.16	7.21	0.14
5	11.02	0.22	10.50	0.21	11.23	0.11	10.96	0.11
10	16.42	0.16	15.50	0.16	16.44	0.08	14.79	0.07
20	24.80	0.12	21.29	0.11	23.23	0.06	22.07	0.06
50	39.10	0.08	36.18	0.07	31.75	0.03	31.46	0.03

In Figs. 8 (a) and (b), damage production efficiency is plotted as a function of Si PKA and C PKA energy in 3C-SiC and 6H-SiC. Although the trend of damage production efficiency is similar to earlier reported results, its magnitude is relatively low.



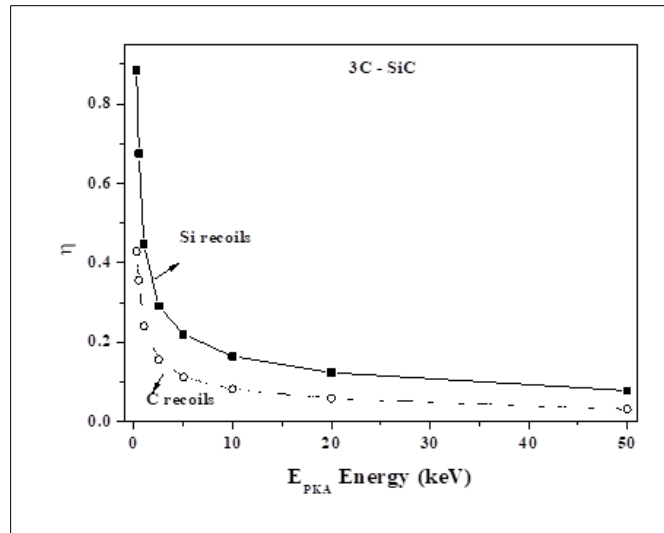


**Figure 8 (a)** Damage production efficiency as a function of Si PKA and C PKA energy in 3C- SiC

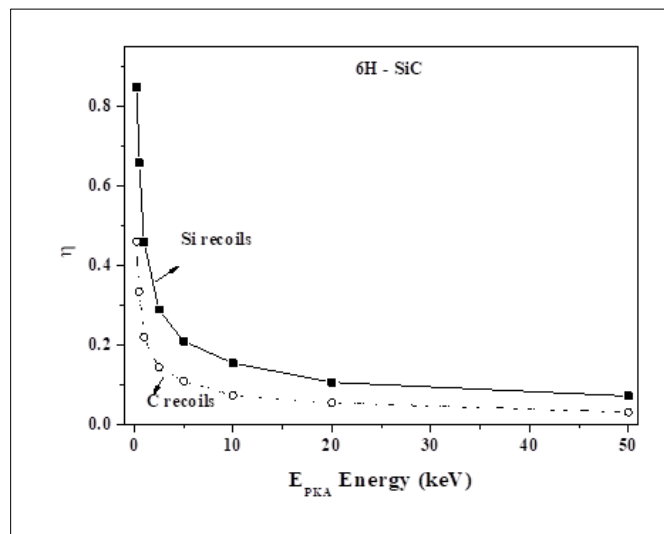


**Figure 8 (b)** Damage production efficiency as a function of Si PKA and C PKA energy in 6H- SiC

Damage production efficiency was also estimated without accounting for electronic energy losses (EEL), revealing that the number of damaged produced, when EEL effects were included, was slightly lower than when EEL effects were not considered. Fig. 9 illustrates the damage production efficiency with and without EEL consideration specifically for 3C-SiC. It can be inferred from the figure that the damage production efficiency tends to be slightly higher when the effect of EEL is not included in the calculations.

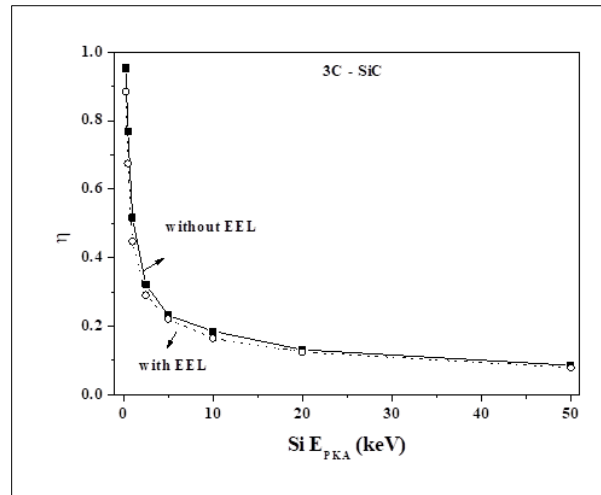


**Figure 9** Damage production efficiency in case of 3C-SiC as a function of Si PKA energy

#### 4. Conclusion

JA-IPU code has been successfully utilized to assess atomic-scale damage production in cubic (3C-SiC) and hexagonal (6H-SiC) SiC polytypes. This computational tool is capable of simulating recoil events up to eight generations. By incorporating four distinct threshold displacement energies for four possible interaction types, the ratio of C interstitials to Si interstitials observed in 3C-SiC is lower compared to previous studies. Specifically, in 3C-SiC, the number of C interstitials exceeds that of Si interstitials, whereas in 6H-SiC, this difference diminishes with increasing PKA energy.

Nevertheless, the number of C vacancies surpass Si vacancies in both the SiC polytypes. When examining damage production efficiency through Si recoils versus C recoils, it is noted that imparting Si recoils tends to yield greater efficiency for both polytypes. The PKA spectrum generated by a fission neutron spectrum in SiC aligns closely with the PKA energy range investigated in this study, underscoring the relevance of the JA-IPU code in the reactor physics research.

#### Compliance with ethical standards

##### *Acknowledgments*

The author is thankful to GGSIP University for providing Indraprastha research fellowship.

##### *Disclosure of conflict of interest*

No conflict of interest to be disclosed.

#### References

- [1] IAEA-TECDOC -1645, High Temperature Gas cooled reactor, International Atomic energy agency, Vienna 2010. ISSN 1684-2073.
- [2] Fenici, P.; Rebelo, A. J. F.; Jones, R. H.; Kohyama, A.; Snead L. L.; J. Nuclear Materials 1998, 258 215-225.
- [3] McHargue, C. J.; Williams, J. M.; Nuclear Instrument Methods Phys. Res. B 1993, 80-81, 889-894.
- [4] Inui, H.; Mori, H.; Fujita, H.; Philos. Mag. B 1990, 61, 107-124.
- [5] Inui, H.; Mori, H.; Sakata, T; Philos. Mag. B 1992, 66, 737.
- [6] Weber, W. J.; Wang, L. M.; Yu, N.; Nuclear Instrument Methods Phys. Res. B 1996, 116, 322.
- [7] Weber, W. J.; Yu, N.; Wang, L. M.; Hess, N. J.; J. Nuclear Materials 1997, 244, 258.
- [8] Grimaldi, M. G.; Calcagno, L.; Musumeci, P.; Frangis, N.; Lunduyt, J. V.; J. Applied. Physics 1997, 81, 7181.

- [9] Wendler, E.; Helt, A.; Wesch, W.; Nuclear Instrument Methods Phys. Res. B 1998, 141, 105.
- [10] Weber, W. J.; Yu, N.; Wang, L. M.; Hess, N. J.; Mater Sci. Engg. A 1998, 253, 62.
- [11] Devanathan, R.; Weber, W. J.; Diaz De La Rubia, T.; Nuclear Instrument Methods Phy Res B 1998, 141, 118.
- [12] Perlado, J. M.; Malerba, L.; Sanchez Rubio, A.; Diaz De La Rubia, T.; J. Nuclear Materials 2000, 276, 235.
- [13] Diaz De La Rubia, T.; Perlado, J. M.; Tobin, M.; J. Nuclear Materials 1996, 233-237, 1096.
- [14] Devanathan, R.; Weber, W. J.; Gao, F.; J. Applied Physics 2001, 90, 2303.
- [15] Gao, F.; Weber, W. J.; Phys Rev. B 2000, 63, 054101.
- [16] Tundwal, A.; Kumar, V.; Kerntechnik 2015, 80 (5), 476-480.
- [17] Zinkle, S.J.; Kinoshita, C.; J. Nuclear Materials 1997, 251, 200-217.
- [18] Broeders, C. H. M.; Konobeyev, A.; Yu., Voukelatou, K.; IOTA- a code to study ion transport and radiation damage in composite materials 2004, 1-2